PNAS
www.pnas.org

Supplementary Information for

GABAergic Synapses Suppress Intestinal Innate Immunity *via* Insulin Signaling in *Caenorhabditis elegans*

Zhongfan Zheng[a,1], Xiumei Zhang[a,1], Junqiang Liu[a,1], Ping He[a,1], Shan Zhang[a], Yongning Zhang[b], Jie Gao[a], Shengmei Yang[a], Na Kang[a], Muhammad Irfan Afridi[a], Shangbang Gao[b], Chunhong Chen[a,c], and Haijun Tu[a,c,2]

[a] State Key Laboratory of Chemo/Biosensing and Chemometrics, College of Biology, Hunan University, 410082 Changsha, Hunan, China
[b] Key Laboratory of Molecular Biophysics of the Ministry of Education, College of Life Science and Technology, Huazhong University of Science and Technology, 430074 Wuhan, Hubei, China
[c]Shenzhen Research Institute, Hunan University, 518000, Shenzhen, Guangdong, China

[1] Z.Z., X.Z., J.L., and P.H. contributed equally to this work.
[2] To whom correspondence may be addressed. **Email:** haijuntu@hnu.edu.cn

This PDF file includes:

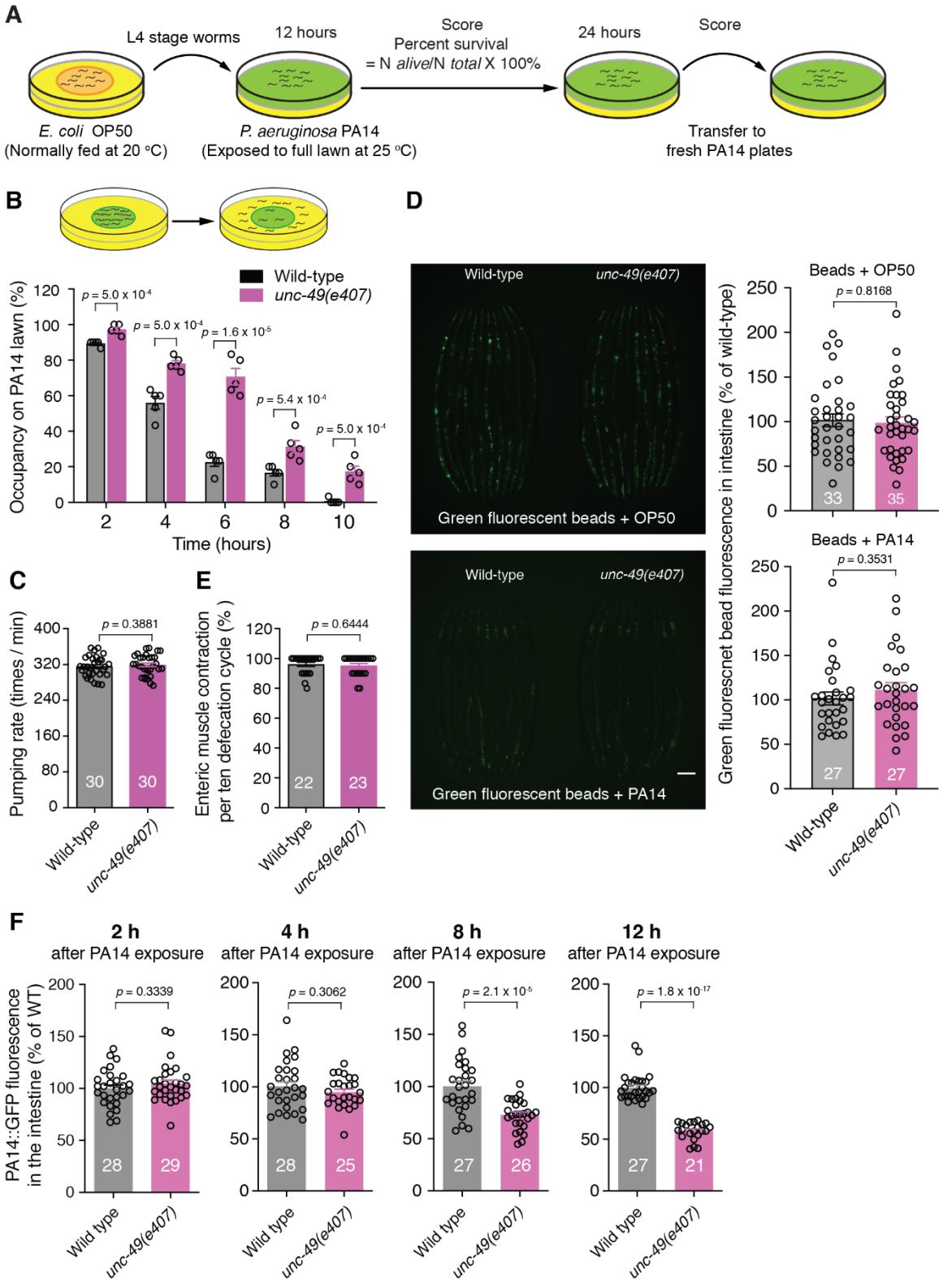

Fig. S1. The effect of deficiency in GABAergic transmission on pathogen avoidance, pumping rate, intakes of food and green fluorescent beads and enteric muscle contraction of *C. elegans*. A. Schematic of the slow killing assay upon a full lawn of *P. aeruginosa* PA14

exposure on nematode growth plate (NGM). **B**. Schematic, and time course of *P. aeruginosa* PA14 lawn occupancy of wild-type, *unc-49(e407)* worms on a small spot of PA14 in a 3.5-cm NGM plate over time. Statistical significance was determined by using one way ANOVA with Bonferroni post-test. The experiment was repeated at least three times independently. **C**. Pumping rate of wild-type, *unc-49(e407)* animals. **D**. Representative images (left) and quantitative analysis (right) of GFP beads accumulated in the intestines of wild-type and *unc-49(e407)* mutant examined by using intake assay of OP50 or PA14 with green fluorescent beads. **E**. The percentage of enteric muscle contracting per ten defecation cycle of wild-type, *unc-49(e407)* worms. **F**. The intensity of PA14::GFP fluorescence in the intestine of wild type and *unc-49(e407)* mutant at different time points after PA14 exposure. Statistical significance was determined by non-paired two-tailed student's *t* test (**B** and **D**), or non-paired Mann-Whitney test (**C**, **E**, and **F**). The number of animals analysed is indicated. The experiments were repeated at least three times independently. Data are presented as means ± SEM. Scale bar indicates 100 μm.

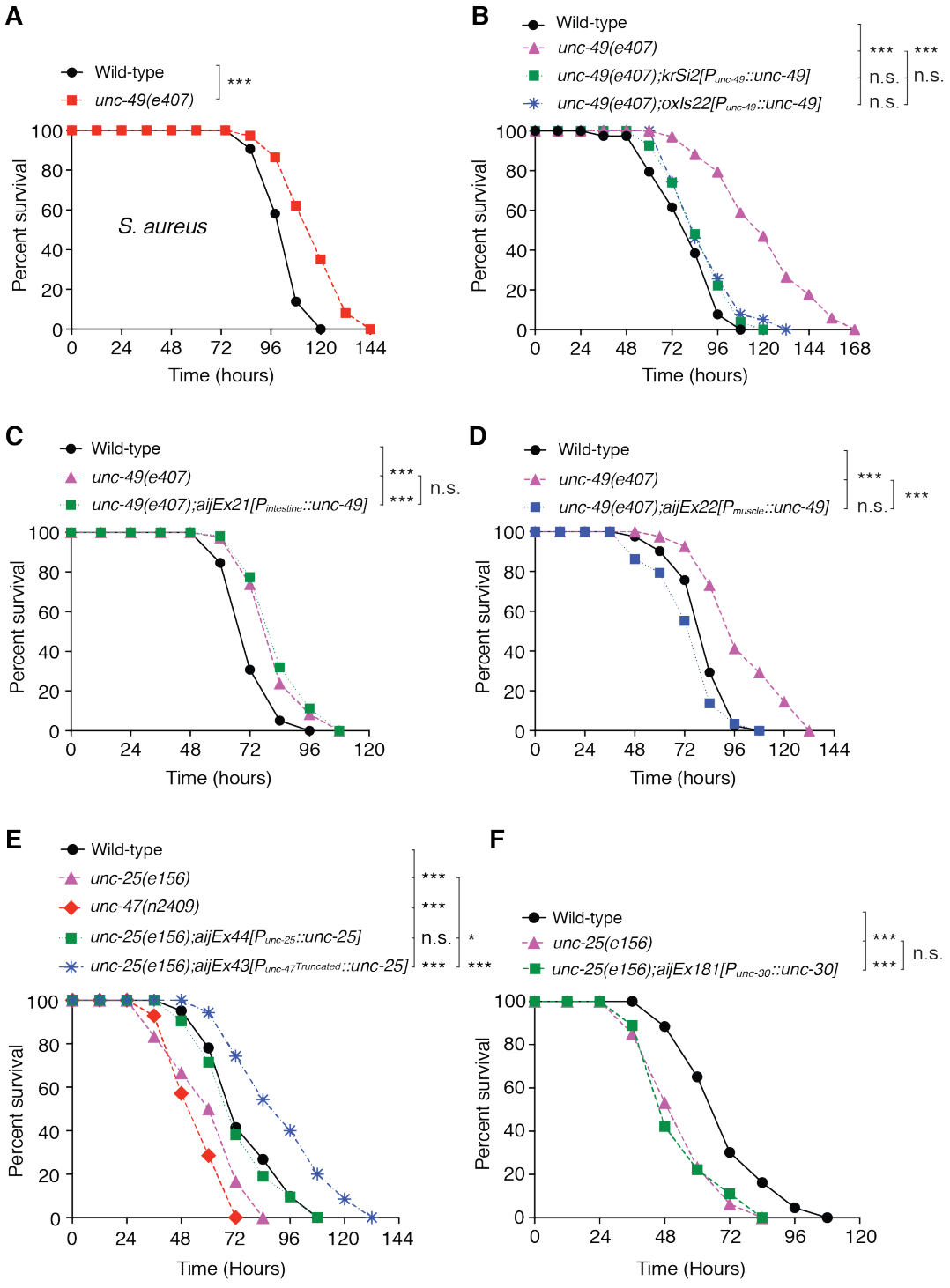

Fig. S2. Loss of GABAergic transmission in D type motor neurons exhibited enhanced resistance to pathogenic PA14 exposure. **A**. Survival of wild-type, *unc-49(e407)* worms exposed to gram-positive *S. aureus*. **B**-**D**. Survival of wild-type, *unc-49(e407)*, or transgenes each carrying a single integrated copy (*krSi2[Punc-49::unc-49B MosSCI]*), or multiple integrated copies (*oxIs22[Punc-49::unc-49::GFP]*) (**B**), or transgenes each overexpressing UNC-49B under the control of *ges-1* (intestine) (**C**), or *myo-3* (muscle) (**D**) promoter in *unc-49(e407)* worms exposed to *P. aeruginosa* PA14. **E**. Survival of wild-type, *unc-25(e156)*, *unc-47(n2409)* and transgene

expressing UNC-25 under the control of its endogenous promoter, or the *unc-47* truncated promoter (driving gene expressed in GABAergic non D-type motor neurons) in *unc-25(e156)* worms exposed to *P. aeruginosa* PA14, respectively. In the transgene *unc-25(e156);aijEx43[Punc-47$_{truncated}$::unc-25]*, the animals only lose function of UNC-25 in D-type motor neurons. **F.** Survival of wild-type, *unc-25(e156)*, and transgene expressing UNC-25 under the control of D-type motor neuron promoter *unc-30* in *unc-25(e156)* worms exposed to *P. aeruginosa* PA14, respectively. Statistical significance was determined by log-rank test for survival assays. *$p < 0.05$, ***$p < 0.001$, n.s., not significant. All the experiments were repeated at least three times independently. The exact *p* values of statistics for all survival assay are listed in Table S1.

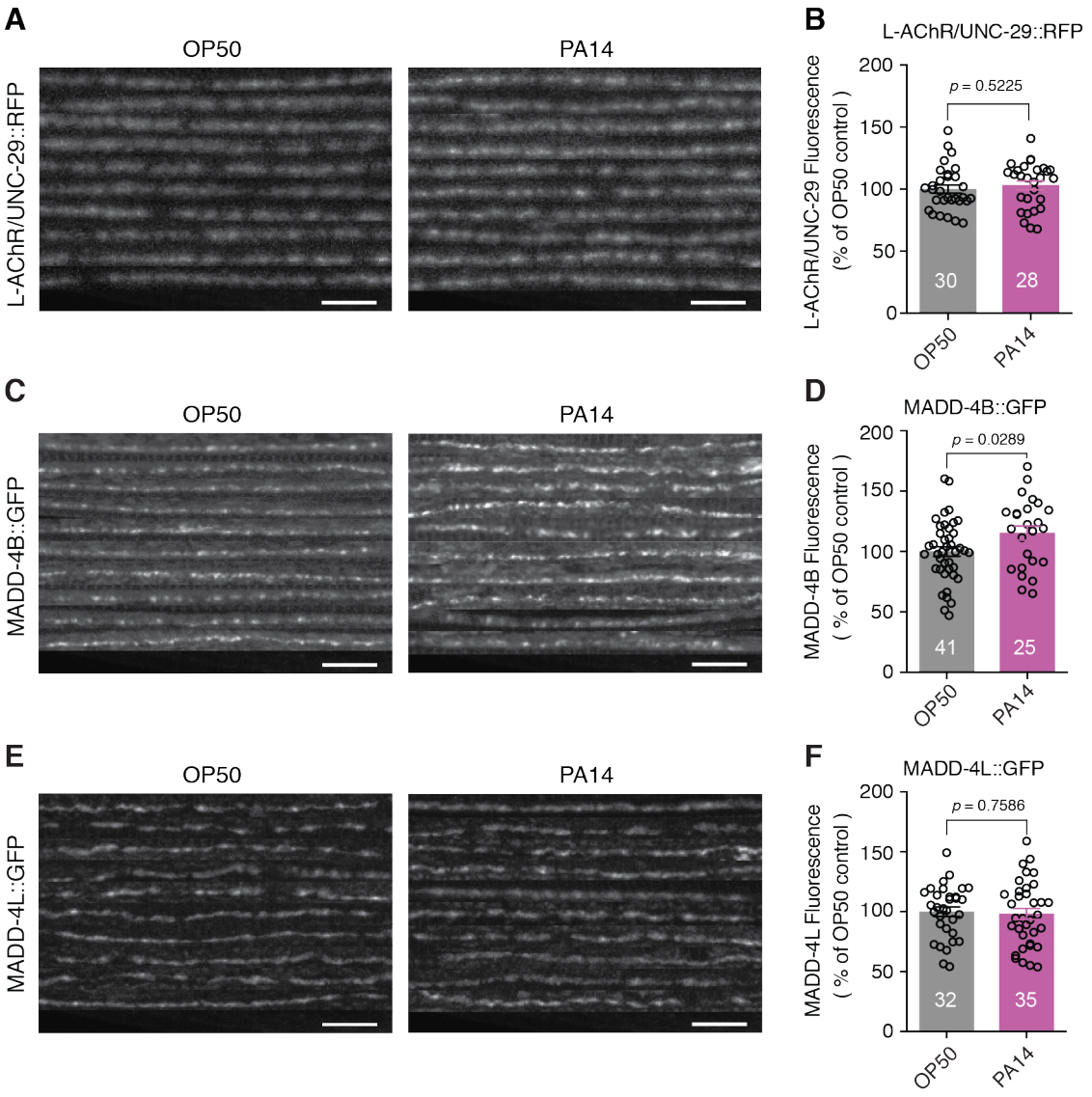

Fig. S3. The effect of pathogenic infection on postsynaptic L-AChR/UNC-29, extracellular matrix MADD-4B and MADD-4L isoforms at nerve cord of worms. A and **B**. Ten representative images (**A**) and fluorescence intensity (**B**) of the L-AChR subunit UNC-29::RFP at the dorsal nerve cord of wild-type worms fed on *E. coli* OP50 or exposed to *P. aeruginosa* PA14. **C-F**. Ten representative images (**C** and **E**) and fluorescence intensity (**D** and **F**) of MADD-4B::GFP (**C** and **D**) or MADD-4L::GFP (**E** and **F**) at the dorsal nerve cord of wild-type worms fed on *E. coli* OP50 or exposed to *P. aeruginosa* PA14, respectively. Statistical significance was determined by non-paired two-tailed student's *t* test (**B**, **D** and **F**). The number of animals analysed is indicated. All the experiments were repeated at least three times independently. Scale bar indicates 10 μm.

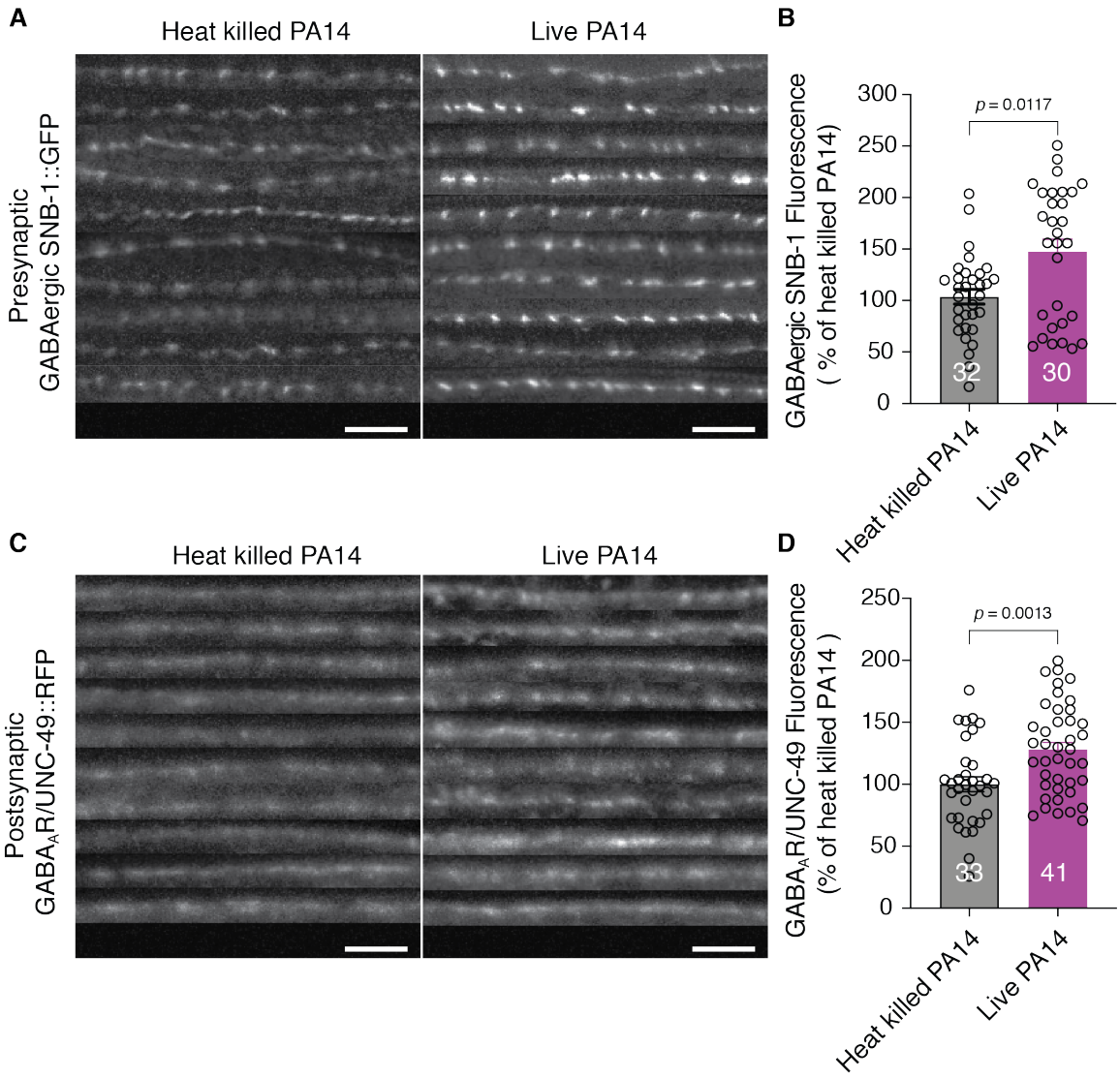

Fig. S4. The effect of live or heat-killed PA14 on the expression of GABAergic presynaptic SNB-1 and postsynaptic GABAAR/UNC-49. A-D. Ten representative images (**A** and **C**) and fluorescence intensity (**B** and **D**) of presynaptic GABAergic SNB-1::GFP (**A** and **B**) and postsynaptic GABA$_A$R/UNC-49::RFP (**C** and **D**) in wild-type animals upon live or heat-killed PA14 exposure, respectively. Statistical significance was determined by non-paired Mann-Whitney test (**B** and **D**). The number of animals analysed is indicated. All the experiments were repeated at least three times independently. Scale bar indicates 10 μm.

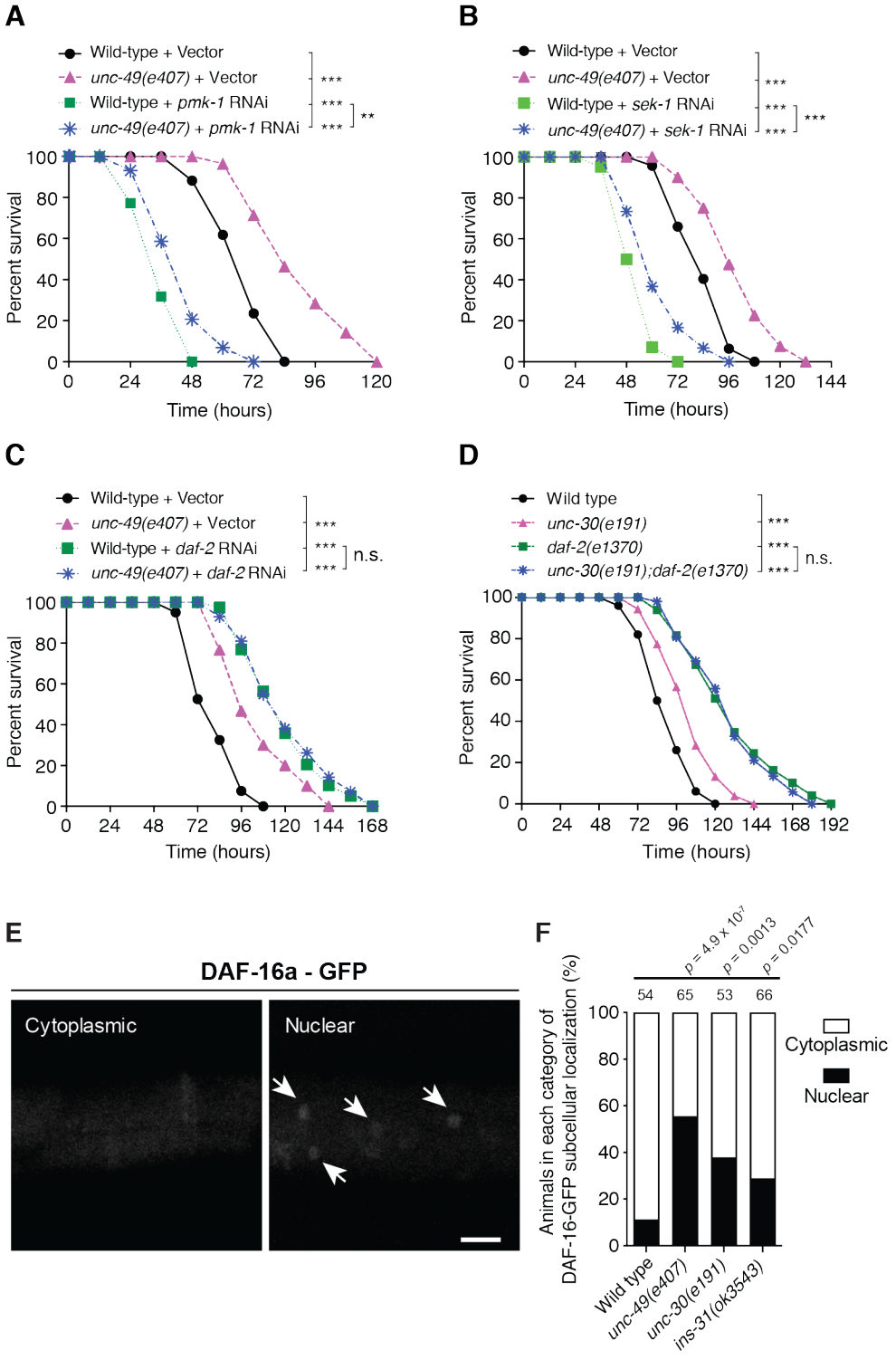

Fig. S5. GABA$_A$R/UNC-49-mediated enhanced resistance to PA14 infection required IIS, but not PMK-1 signaling. A-C. Survival of wild-type and *unc-49(e407)* animals on control or *daf-2* RNAi (**A**), or *pmk-1* RNAi (**B**), or *sek-1* RNAi (**C**) exposed to *P. aeruginosa* PA14. **D.** Survival of wild-type, *unc-30(e191)*, *daf-2(e1370)*, or *unc-30(e191);daf-2(e1370)* double mutant animals exposed to *P. aeruginosa* PA14, respectively. **E** and **F**. The representative images of two

categories (**E**) and quantification analysis (**F**) of nuclear accumulation of DAF-16a–GFP in wild-type, *unc-49(e407), unc-30(e191), and ins-31(ok3543)* mutant animals, respectively. Statistical significance was determined by log-rank test for survival assays or Chi-square for (**F**). ***p* < 0.01, ****p* < 0.001, n.s., not significant. Scale bar indicates 20 μM. All the experiments were repeated at least three times independently. The exact *p* values of statistics for all survival assay are in Table S1.

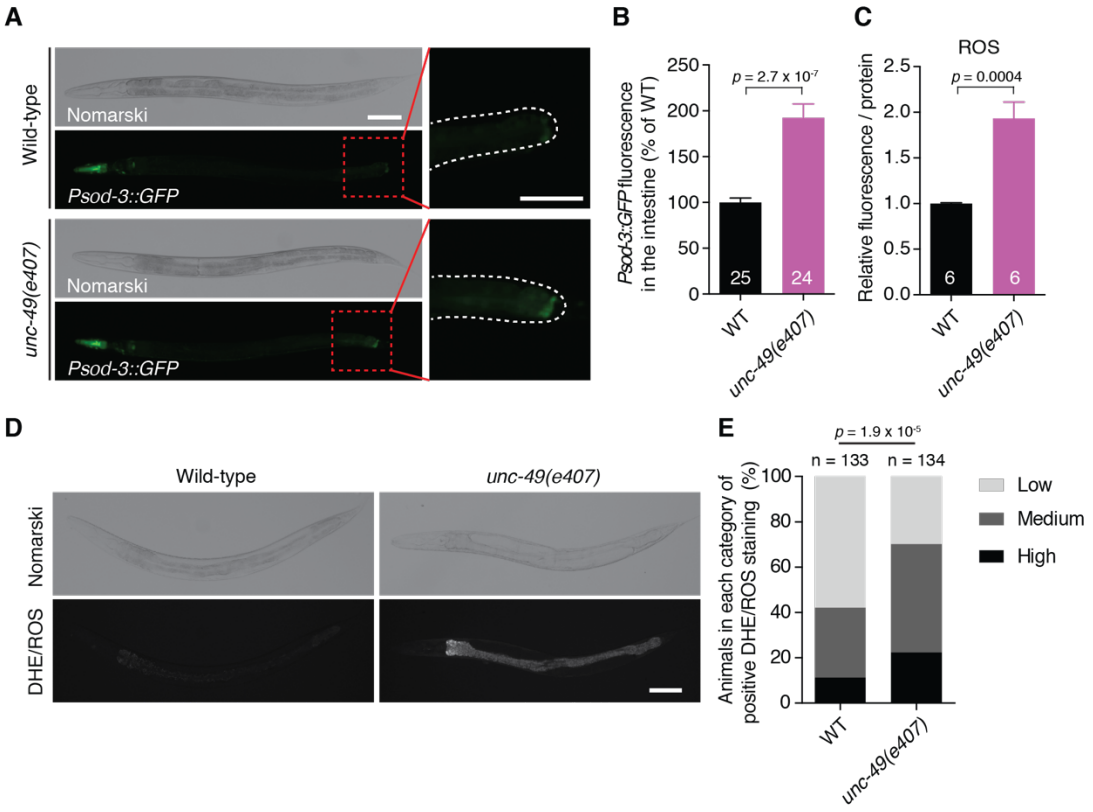

Figure S6. Loss function of *unc-49* upregulates DAF-16 activity marker SOD-3 and ROS levels in the intestine of worms. A and **B**. Representative images (**A**) and quantification (**B**) of transcriptional SOD-3::GFP reporter in the intestine of wild type and *unc-49(e407)* worms. **C**. Quantitative analysis of ROS level in whole worm lysates of wild type and *unc-49(e407)*. Statistical significance was determined by non-paired two-tailed student's t-test (**B** and **C**). **D** and **E**. Representative images (**D**) and quantification (**E**) of DHE/ROS staining in wild type and *unc-49(e407)*, respectively. Statistical significance was determined by the Chi-square. Scale bar indicates 100 μM. The number of animals analysed is indicated. All the experiments were repeated at least three times independently.

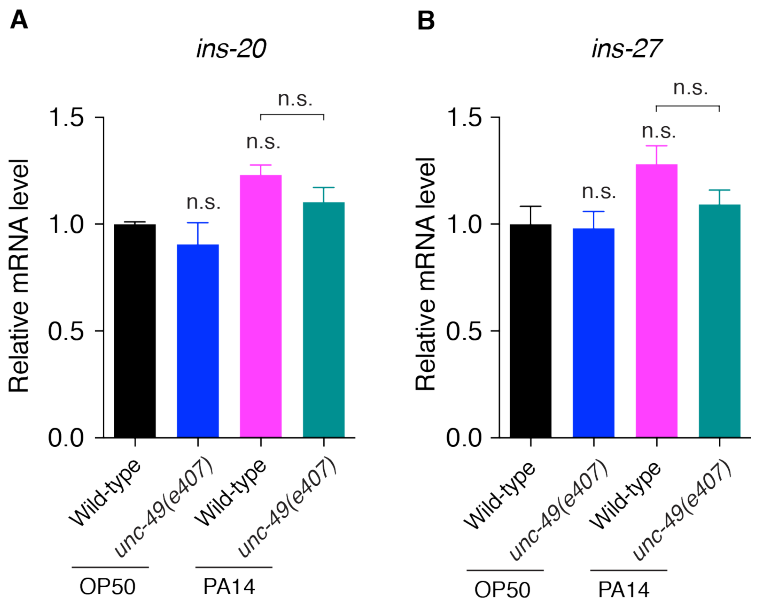

Fig. S7. Quantitative RT-PCR analyses of *ins-20* (A) and *ins-27* (B) mRNA level in wild type or *unc-49(e407)* animals fed on OP50 or exposed to PA14, respectively, showing the loss-function of GABAAR/UNC-49 does not affect their expression. Statistical significance was determined by non-paired two-tailed student's *t* test. n.s., not significant. The exact *p* values of statistics for quantitative real time PCR are listed in Table S2.

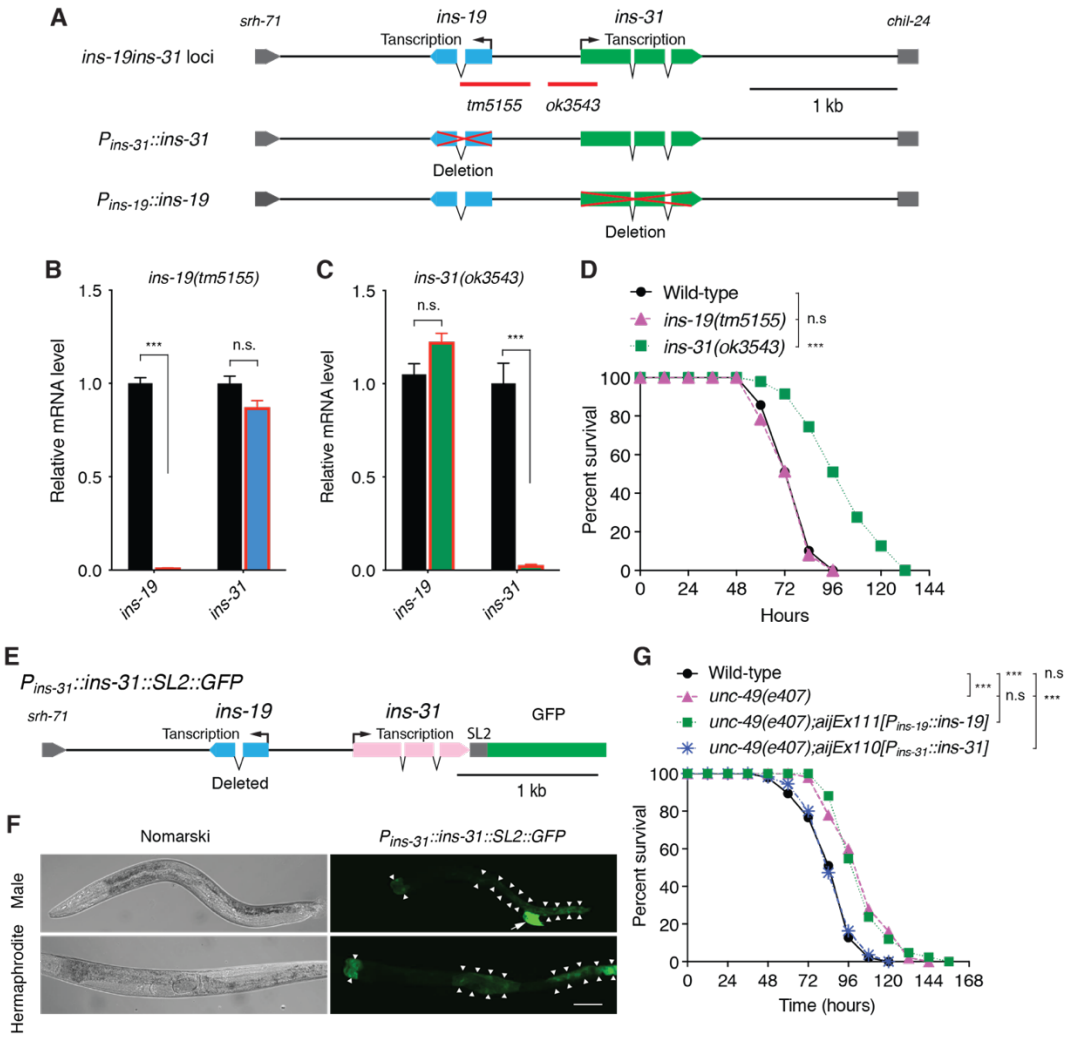

Fig. S8. Insulin/insulin-like peptide INS-31 acts downstream of GABAergic transmission although it is highly expressed in seminal vesicle of male gonad and intestine. A. Schematic diagram of *ins-19* and *ins-31* genes organization showing *ins-19* and *ins-31* loci, *tm5155* deletion allele of *ins-19*, *ok3543* deletion allele of *ins-31*, the *Pins-31::ins-31* construction with *ins-19* deletion region, and *Pins-19::ins-19* construction with *ins-31* deletion. **B** and **C**. Quantitative RT-PCR analyses of *ins-19* and *ins-31* expression level in *ins-19(tm5155)* or in *ins-31(ok3543)* worms showing the alleles, *tm5155* and *ok3543*, affect the expression of *ins-19* and *ins-31*, respectively. Statistical significance was determined by non-paired two-tailed student's *t* test. ***$p < 0.001$, n.s., not significant. **D.** Survival of wild-type, *ins-19(tm5155)* and *ins-31(ok3542)* mutants showing only *ins-31*, but not *ins-19* exhibited enhanced resistance to PA14 exposure. **E** and **F**. Schematic diagram (E) and representative images (F) of GFP expressing trans-spliced by SL2 under the control of *ins-31* promoter (*Pins-31::ins-31::SL2::GFP*) showing *ins-31* expresses in seminal vesicle of male gonad (arrow) and in intestine (arrow head). Scale bar, 10 μm. **G**. Survival of wild-type, *unc-49(e407)* and transgenes carrying *ins-19* (*aijEx111[Pins-19::ins-19]*) or *ins-31* (*aijEx110[Pins-31::ins-31]*) locus in *unc-49(e407)* worms exposed to PA14, respectively. Statistical significance was determined by log-rank test for survival assays, or unpaired Student's *t* test for (**C** and **D**). *$p < 0.05$, ***$p < 0.001$, n.s., not significant. The exact *p* values of statistics for all survival assay and quantitative real time PCR are listed in Table S1 and S2, respectively.

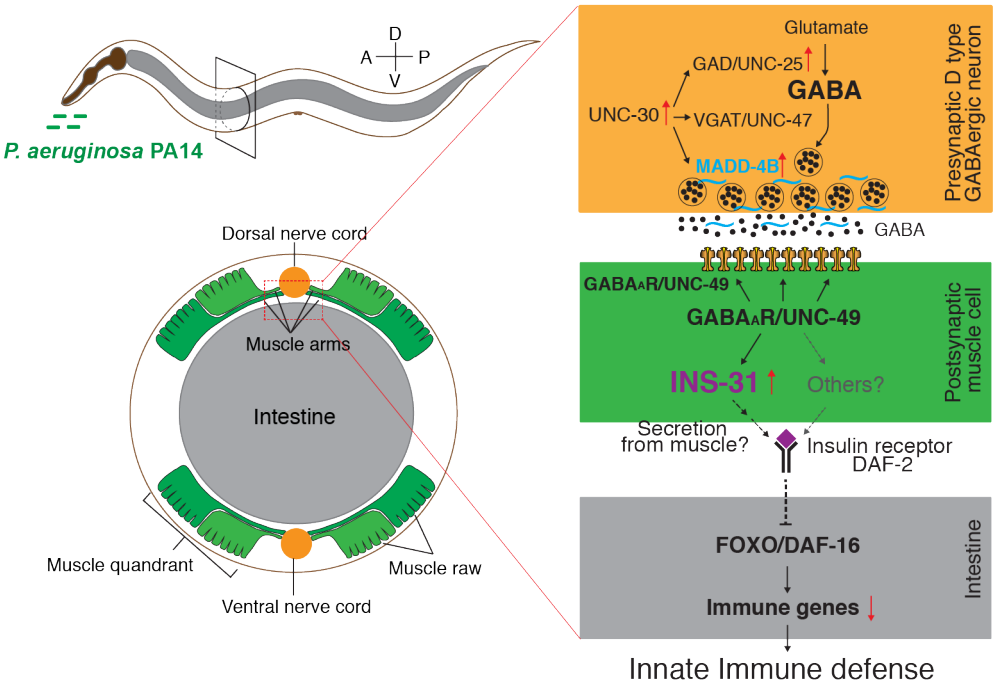

Fig. S9. Working model of GABAergic neurotransmission suppresses intestinal innate immunity *via* insulin-like Signalling.

Table S1. Statistics for survival assay.

Strain (Genotype)	TD mean ± SEM (hours)	# Worms Scored/Total	P value	Figure
WT	75.20 ± 1.38	45/50		Fig. 1A
unc-49 (e382)	84.00 ± 1.76	42/50	$p = 3.1 \times 10^{-9}$ vs WT	
unc-49 (e407)	88.38 ± 1.42	52/60	p = 0.0002 vs WT	
WT	80.93 ± 1.43	43/50		Fig. 1B
unc-49 (e407)	102.30 ± 2.47	40/50	$p = 6.2 \times 10^{-11}$ vs WT	
gbb-1 (tm1406)	84.44 ± 1.75	54/60	p = 0.0663 vs WT	
gbb-2 (tm1165)	77.57 ± 1.39	56/60	p = 0.1523 vs WT	
WT (heat-killed PA14)	16.70 ± 0.61 Days	30/50		Fig. 1C
unc-49(e407) (heat-killed PA14)	16.31 ± 0.65 Days	32/50	p = 0.7248	
WT	71.52 ± 1.48	50/50		Fig. 1I
unc-49(e407)	87.07 ± 1.98	43/50	$p = 4.1 \times 10^{-8}$ vs WT	
unc-49(e407);krSi2[Punc-49::unc-49]	74.79 ± 1.67	43/50	p = 0.1425 vs WT, $p = 2.2 \times 10^{-5}$ vs *unc-49(e407)*	
WT	84.00 ± 1.56	36/50		Fig. 1J
unc-49(e407)	100.80 ± 2.15	45/50	$p = 2.0 \times 10^{-8}$ vs WT	
unc-49(e407);aijSi1[Pmuscle::unc-49]	85.89 ± 1.87	38/50	p = 0.3275 vs WT, $p = 1.7 \times 10^{-6}$ vs *unc-49(e407)*	
unc-49(e407);aijSi2[Pintestine::unc-49]	102.32 ± 2.31	38/50	$p = 1.5 \times 10^{-8}$ vs WT, p = 0.6996 vs *unc-49(e407)*	
WT	76.31 ± 2.44	27/50		Fig. 1L
unc-30(e191)	86.00 ± 2.89	43/50	$p = 2.2 \times 10^{-6}$ vs WT	
aijSi11[Punc-30-Tetx]	97.16 ± 2.59	31/50	$p = 2.6 \times 10^{-6}$ vs WT	
WT	82.04 ± 1.74	49/60		Fig. 1N
unc-25(e156)	67.47 ± 2.11	45/60	$p = 9.4 \times 10^{-6}$ vs WT	
unc-25(e156);aijEx42[Punc-47$_{Truncated}$::unc-25]	97.28 ± 2.40	47/60	$p = 3.0 \times 10^{-6}$ vs WT, $p = 2.8 \times 10^{-15}$ vs *unc-25(e156)*	
unc-25(e156);aijEx143[Punc-30::unc-25]	59.18 ± 1.87	44/60	$p = 1.7 \times 10^{-11}$ vs WT, p = 0.0053 vs *unc-25(156)*	
WT	79.06 ± 2.11	51/60		Fig. 3A
unc-49(e407)	93.96 ± 2.83	47/60	$p = 4.9 \times 10^{-5}$ vs WT	
daf-16(mu86)	79.92 ± 2.14	50/60	p = 0.7879 vs WT	
unc-49(e407);daf-16(mu86)	79.57 ± 2.00	46/60	p = 0.9814 vs WT, $p = 4.9 \times 10^{-5}$ vs *unc-49(e407)*	
WT	92.84 ± 2.99	38/50		Fig. 3B
unc-49(e407)	114.58 ± 3.18	31/50	$p = 8.3 \times 10^{-6}$ vs WT	
daf-2(e1370)	147.09 ± 5.30	35/50	$p = 3.3 \times 10^{-14}$ vs WT	
unc-49(e407);daf-2(e1370)	138.67 ± 6.20	27/50	$p = 5.2 \times 10^{-10}$ vs WT, p = 0.3238 vs *daf-2(e1370)*	
WT	82.63 ± 2.46	35/50		Fig. 3C
unc-49(e407)	99.22 ± 2.52	41/50	$p = 4.1 \times 10^{-5}$ vs WT	
age-1(hx546)	127.20 ± 4.94	25/50	$p = 3.9 \times 10^{-10}$ vs WT	
unc-49(e407);age-1(hx546)	124.80 ± 4.10	30/50	$p = 2.0 \times 10^{-11}$ vs WT, p = 0.6134 vs *age-1(hx546)*	
WT	76.39 ± 1.54	41/50		Fig. 4A
unc-49(e407)	84.33 ± 1.97	36/50	p = 0.0028 vs WT	
pmk-1(km25)	51.92 ± 1.22	49/50	$p = 1.9 \times 10^{-16}$ vs WT	
unc-49(e407);pmk-1(km25)	59.47 ± 1.96	45/50	$p = 2.3 \times 10^{-7}$ vs WT, p = 0.0009 vs *pmk-1(km25)*	
WT	77.82 ± 2.36	33/50		Fig. 4B
unc-49(e407)	94.33 ± 2.61	43/50	$p = 9.9 \times 10^{-6}$ vs WT	
nsy-1(ag-3)	48.92 ± 1.53	39/50	$p = 7.1 \times 10^{-13}$ vs WT	
unc-49(e407);nsy-1(ag3)	61.82 ± 2.31	33/50	$p = 2.4 \times 10^{-5}$ vs WT, $p = 2.4 \times 10^{-5}$ vs *nsy-1(ag3)*	
WT	80.00 ± 2.35	27/50		Fig. 4C
unc-49(e407)	97.16 ± 2.76	31/50	$p = 3.8 \times 10^{-5}$ vs WT	
sek-1(km4)	52.22 ± 1.54	37/50	$p = 1.9 \times 10^{-11}$ vs WT	
unc-49(e407);sek-1(km4)	62.32 ± 2.35	31/50	$p = 3.0 \times 10^{-5}$ vs WT, p = 0.0008 vs *sek-1(km4))*	
WT	79.85 ± 1.75	52/60		Fig. 5B
ins-31(ok3543)	97.80 ± 2.11	60/60	$p = 4.5 \times 10^{-9}$	
WT+Vector	81.36 ± 1.84	50/60		Fig. 5B
WT+*ins-31* RNAi	91.59 ± 2.39	49/60	p = 0.0005 vs WT+Vector	
WT	77.49 ± 2.54	35/50		Fig. 5C
ins-31(ok3543)	91.32 ± 2.51	41/50	p = 0.0004 vs WT	
ins-31(ok3543);aijEx135[Pins-31::ins-31]	62.75 ± 2.27	48/50	p = 0.0003 vs WT, $p = 7.8 \times 10^{-11}$ vs *ins-31(ok3543)*	
ins-31(ok3543);aijEx126[Pintestine::ins-31]	90.97 ± 2.83	31/50	p = 0.0011 vs WT, p = 0.9007 vs *ins-31(ok3543)*	
ins-31(ok3543);aijEx132[Pmuscle::ins-31]	69.78 ± 1.89	54/50	p = 0.0176 vs WT, $p = 8.1 \times 10^{-6}$ vs *ins-31(ok3543)*	

Table S1. Continued.

Strain (Genotype)	TD mean ± SEM (hours)	# Worms Scored/Total	P value	Figure
WT	80.00 ± 2.18	27/40		Fig. 6A
unc-49(e407)	108.46 ± 2.88	26/40	$p = 2.3 \times 10^{-9}$ vs WT	
ins-31(ok3543)	95.08 ± 2.52	26/40	p = 0.0001 vs WT	
unc-49(e407);ins-31(ok3543)	108.46 ± 3.03	26/40	$p = 5.3 \times 10^{-9}$ vs WT, p = 0.9498 vs *unc-49(e407)*	
WT	86.51 ± 2.07	43/50		Fig. 6B
unc-49(e407)	103.26 ± 2.66	38/50	$p = 3.7 \times 10^{-6}$ vs WT	
unc-49(e407);aijEx110[Pins-31::ins-31]	89.56 ± 1.66	41/50	$p = 0.4997$ vs WT, $p = 1.6 \times 10^{-5}$ vs *unc-49(e407)*	
WT	81.21 ± 1.52	43/50		Fig. 6C
unc-49(e407)	96.00 ± 2.43	37/50	$p = 7.5 \times 10^{-7}$ vs WT	
unc-49(e407);aijEx88[Pintestine::ins-31]	93.45 ± 2.45	33/50	$p = 4.4 \times 10^{-5}$ vs WT, p = 0.4389 vs *unc-49(e407)*	
unc-49(e407);aijEx89[Pmuscle::ins-31]	80.21 ± 2.00	38/50	$p = 0.8841$ vs WT, $p = 6.8 \times 10^{-6}$ vs *unc-49(e407)*	
WT	84.56 ± 2.12	43/50		Fig. 6H
ins-31(ok3543)	103.32 ± 2.95	41/50	$p = 3.0 \times 10^{-6}$ vs WT	
daf-16(mu86)	86.77 ± 2.02	39/50	p = 0.6214 vs WT	
ins-31(ok3543);daf-16(mu86)	82.67 ± 2.20	36/50	p = 0.4659 vs WT, p = 0.2198 vs *daf-16(mu86)*	
WT	84.00 ± 2.79	37/50		Fig. 6J
ins-31(ok3543)	100.00 ± 2.92	45/50	p = 0.0004 vs WT	
daf-2(e1370)	141.47 ± 4.15	38/50	$p = 3.8 \times 10^{-16}$ vs WT	
ins-31(ok3543);daf-2(e1370)	142.74 ± 3.54	38/50	$p = 2.9 \times 10^{-17}$ vs WT, p = 0.8213 vs *daf-2(e1370)*	
WT (*S.aureus)*	103.53 ± 1.53	43/50		Fig. S2A
unc-49(e407) (S.aureus)	118.70 ± 2.42	37/50	$p = 5.7 \times 10^{-7}$	
WT	81.85 ± 2.64	39/50		Fig. S2B
unc-49(e407)	106.20 ± 5.68	40/50	p = 0.0001 vs WT	
unc-49(e407);krSi2[Punc-49::unc-49]	88.89 ± 2.97	27/50	p = 0.0554 vs WT, p = 0.0058 vs *unc-49(e407)*	
unc-49(e407);oxIs22[Punc-49::unc-49]	91.08 ± 2.64	39/50	p = 0.152 vs WT, p = 0.0041 vs *unc-49(e407)*	
WT	74.46 ± 1.45	39/50		Fig. S2C
unc-49(e407)	83.73 ± 1.79	45/50	p = 0.0002 vs WT	
unc-49(e407);aijEx21[Pintestine::unc-49]	86.26 ± 1.57	53/60	$p = 1.2 \times 10^{-6}$ vs WT, p = 0.3441 vs *unc-49(e407)*	
WT	83.41 ± 1.89	41/50		Fig. S2D
unc-49(e407)	101.85 ± 2.90	41/50	$p = 6.5 \times 10^{-7}$ vs WT	
unc-49(e407);aijEx22[Pmuscle::unc-49]	76.55 ± 2.83	29/50	$p = 0.001$ vs WT, $p = 3.9 \times 10^{-8}$ vs *unc-49(e407)*	
WT	78.15 ± 2.52	41/50		Fig. S2E
unc-25(e156)	62.00 ± 3.29	48/50	p = 0.0005 vs WT	
unc-47(n2409)	57.43 ± 3.01	42/50	$p = 7.9 \times 10^{-6}$ vs WT	
unc-25(e156);aijEx44[Punc-25::unc-25]	75.43 ± 3.63	42/50	p = 0.6055 vs WT, p = 0.0166 vs *unc-25(e156)*	
unc-25(e156);aijEx43[Punc-47$_{Truncated}$::unc-25]	94.97 ± 3.48	35/50	p = 0.0002 vs WT, $p = 1.7 \times 10^{-8}$ vs *unc-25(e156)*	
WT	72.56 ± 2.40	43/50		Fig. S2F
unc-25(e156)	56.17 ± 1.95	47/50	$p = 2.8 \times 10^{-6}$ vs WT	
unc-25(e156);aijEx181[Punc-30::unc-30]	55.73 ± 2.07	45/50	$p = 6.0 \times 10^{-6}$ vs WT, p = 0.9981 vs *unc-25(e156)*	
WT+Vector	92.82 ± 1.95	34/50		Fig. S5A
unc-49(e407)+Vector	114.86 ± 3.29	28/50	$p = 6.3 \times 10^{-7}$ vs WT+Vector	
WT+*pmk-1* RNAi	61.09 ± 1.88	22/50	$p = 2.4 \times 10^{-13}$ vs WT+Vector	
unc-49(e407)+*pmk-1* RNAi	69.52 ± 2.22	29/50	$p = 3.5 \times 10^{-9}$ vs WT+Vector, p = 0.008 vs WT+*pmk-1* RNAi	
WT+Vector	85.02 ± 1.80	47/50		Fig. S5B
unc-49(e407)+Vector	101.10 ± 2.61	40/50	$p = 1.8 \times 10^{-6}$ vs WT+Vector	
WT+*sek-1* RNAi	54.29 ± 1.29	42/50	$p = 5.5 \times 10^{-19}$ vs WT+Vector	
unc-49(e407)+*sek-1* RNAi	64.00 ± 2.55	30/50	$p = 3.6 \times 10^{-8}$ vs WT+Vector, p = 0.0007 vs WT+*sek-1* RNAi	
WT+Vector	82.50 ± 2.04	40/50		Fig. S5C
unc-49(e407)+Vector	101.78 ± 2.97	27/50	$p = 9.6 \times 10^{-6}$ vs WT+Vector	
WT+*daf-2* RNAi	120.31 ± 3.38	39/50	$p = 6.5 \times 10^{-14}$ vs WT+Vector	
unc-49(e407)+*daf-2* RNAi	121.71 ± 3.58	42/50	$p = 2.5 \times 10^{-14}$ vs WT+Vector, p = 0.6818 vs WT+*daf-2* RNAi	
WT	91.20 ± 2.09	50/60		Fig. S5D
unc-30(e156)	104.83 ± 2.44	53/60	p = 0.0001 vs WT	
daf-2(e1370)	130.04 ± 4.12	49/60	$p = 7.6 \times 10^{-14}$ vs WT	
unc-30(e156);daf-2(e1370)	129.23 ± 3.51	52/60	$p = 6.2 \times 10^{-14}$ vs WT, p = 0.6376 vs *daf-2(e1370)*	
WT	77.63 ± 1.47	49/50		Fig. S8D
ins-19(tm5155)	76.54 ± 1.80	37/50	p = 0.7432 vs WT	
ins-31(ok3543)	102.64 ± 2.65	47/50	$p = 1.8 \times 10^{-12}$ vs WT	

Table S1. Continued.

Strain (Genotype)	TD mean ± SEM (hours)	# Worms Scored/Total	P value	Figure
unc-49(e407)	105.84 ± 2.39	50/60	$p = 2.8 \times 10^{-7}$ vs WT	
unc-49(e407);aijEx111[Pins-19::ins-19]	106.29 ± 2.48	42/60	$p = 5.4 \times 10^{-7}$ vs WT, p = 0.9834 vs *unc-49(e407)*	
unc-49(e407);aijEx110[Pins-31::ins-31]	88.80 ± 1.94	55/60	p = 0.7884 vs WT, $p = 3.4 \times 10^{-7}$ vs *unc-49(e407)*	

Table S2. The exact *p* values of statistics for quantitative real time PCR.

Target gene	Strain and treatment comparison	*p* value	Figure
abf-2	WT OP50 fed vs *unc-49(e407)* OP50 fed	8.0×10^{-5}	Fig. 3D
	WT OP50 fed vs WT PA14 exposed	0.0019	
	WT PA14 exposed vs *unc-49(e407)* PA14 exposed	9.0×10^{-6}	
ctl-2	WT OP50 fed vs *unc-49(e407)* OP50 fed	0.005	
	WT OP50 fed vs WT PA14 exposed	1.8×10^{-4}	
	WT PA14 exposed vs *unc-49(e407)* PA14 exposed	0.016	
dod-22	WT OP50 fed vs *unc-49(e407)* OP50 fed	0.0064	
	WT OP50 fed vs WT PA14 exposed	4.1×10^{-21}	
	WT PA14 exposed vs *unc-49(e407)* PA14 exposed	1.1×10^{-17}	
mtl-1	WT OP50 fed vs *unc-49(e407)* OP50 fed	3.3×10^{-7}	
	WT OP50 fed vs WT PA14 exposed	0.0045	
	WT PA14 exposed vs *unc-49(e407)* PA14 exposed	0.0114	
sod-3	WT OP50 fed vs *unc-49(e407)* OP50 fed	3.3×10^{-9}	
	WT OP50 fed vs WT PA14 exposed	0.0006	
	WT PA14 exposed vs *unc-49(e407)* PA14 exposed	2.1×10^{-11}	
thn-2	WT OP50 fed vs *unc-49(e407)* OP50 fed	0.0014	
	WT OP50 fed vs WT PA14 exposed	2.1×10^{-5}	
	WT PA14 exposed vs *unc-49(e407)* PA14 exposed	0.0242	
abf-2	WT PA14 exposed vs *unc-49(e407)* PA14 exposed	1.9×10^{-7}	Fig. 3E
	unc-49(e407) PA14 exposed vs *unc-49(e407);krSi2[Punc-49::unc-49]* PA14 exposed	3.8×10^{-5}	
	unc-49(e407) PA14 exposed vs *unc-49(e407);aijSi1[Pmyo-3::unc-49]* PA14 exposed	3.0×10^{-6}	
	unc-49(e407) PA14 exposed vs *unc-49(e407);aijSi2[Pges-1::unc-49]* PA14 exposed	1	
ctl-2	WT PA14 exposed vs *unc-49(e407)* PA14 exposed	7.0×10^{-6}	
	unc-49(e407) PA14 exposed vs *unc-49(e407);krSi2[Punc-49::unc-49]* PA14 exposed	5.0×10^{-6}	
	unc-49(e407) PA14 exposed vs *unc-49(e407);aijSi1[Pmyo-3::unc-49]* PA14 exposed	1.2×10^{-5}	
	unc-49(e407) PA14 exposed vs *unc-49(e407);aijSi2[Pges-1::unc-49]* PA14 exposed	1	
dod-22	WT PA14 exposed vs *unc-49(e407)* PA14 exposed	0.0008	
	unc-49(e407) PA14 exposed vs *unc-49(e407);krSi2[Punc-49::unc-49]* PA14 exposed	0.0243	
	unc-49(e407) PA14 exposed vs *unc-49(e407);aijSi1[Pmyo-3::unc-49]* PA14 exposed	0.0002	
	unc-49(e407) PA14 exposed vs *unc-49(e407);aijSi2[Pges-1::unc-49]* PA14 exposed	0.0193	
mtl-1	WT PA14 exposed vs *unc-49(e407)* PA14 exposed	6.9×10^{-5}	
	unc-49(e407) PA14 exposed vs *unc-49(e407);krSi2[Punc-49::unc-49]* PA14 exposed	0.0004	
	unc-49(e407) PA14 exposed vs *unc-49(e407);aijSi1[Pmyo-3::unc-49]* PA14 exposed	0.0184	
	unc-49(e407) PA14 exposed vs *unc-49(e407);aijSi2[Pges-1::unc-49]* PA14 exposed	0.4476	
sod-3	WT PA14 exposed vs *unc-49(e407)* PA14 exposed	0.0012	
	unc-49(e407) PA14 exposed vs *unc-49(e407);krSi2[Punc-49::unc-49]* PA14 exposed	0.004	
	unc-49(e407) PA14 exposed vs *unc-49(e407);aijSi1[Pmyo-3::unc-49]* PA14 exposed	0.008	
	unc-49(e407) PA14 exposed vs *unc-49(e407);aijSi2[Pges-1::unc-49]* PA14 exposed	1	
thn-2	WT PA14 exposed vs *unc-49(e407)* PA14 exposed	2.3×10^{-5}	
	unc-49(e407) PA14 exposed vs *unc-49(e407);krSi2[Punc-49::unc-49]* PA14 exposed	0.0047	
	unc-49(e407) PA14 exposed vs *unc-49(e407);aijSi1[Pmyo-3::unc-49]* PA14 exposed	0.0016	
	unc-49(e407) PA14 exposed vs *unc-49(e407);aijSi2[Pges-1::unc-49]* PA14 exposed	0.639	

Table S2. Continued.

Target gene	Strain and treatment comparison	*p* value	Figure
F35E12.5	WT OP50 fed vs *unc-49(e407)* OP50 fed	1	Fig. 4D
	WT OP50 fed vs WT PA14 exposed	0.0003	
	WT PA14 exposed vs *unc-49(e407)* PA14 exposed	1	
F08G5.6	WT OP50 fed vs *unc-49(e407)* OP50 fed	1	
	WT OP50 fed vs WT PA14 exposed	4.2×10^{-7}	
	WT PA14 exposed vs *unc-49(e407)* PA14 exposed	0.2042	
K08D8.5	WT OP50 fed vs *unc-49(e407)* OP50 fed	1	
	WT OP50 fed vs WT PA14 exposed	0.0075	
	WT PA14 exposed vs *unc-49(e407)* PA14 exposed	1	
lys-1	WT OP50 fed vs *unc-49(e407)* OP50 fed	1	
	WT OP50 fed vs WT PA14 exposed	1.9×10^{-7}	
	WT PA14 exposed vs *unc-49(e407)* PA14 exposed	1	
lys-2	WT OP50 fed vs *unc-49(e407)* OP50 fed	1	
	WT OP50 fed vs WT PA14 exposed	5.0×10^{-6}	
	WT PA14 exposed vs *unc-49(e407)* PA14 exposed	1	
clec-85	WT OP50 fed vs *unc-49(e407)* OP50 fed	1	
	WT OP50 fed vs WT PA14 exposed	6.8×10^{-5}	
	WT PA14 exposed vs *unc-49(e407)* PA14 exposed	1	
ins-31	WT PA14 exposed vs *unc-49(e407)* PA14 exposed	2.8×10^{-7}	Fig. 5A
	unc-49(e407) PA14 exposed vs *unc-49(e407);krSi2[Punc-49::unc-49]* PA14 exposed	4.6×10^{-7}	
	unc-49(e407) PA14 exposed vs *unc-49(e407);aijSi1[Pmyo-3::unc-49]* PA14 exposed	0.0002	
	unc-49(e407) PA14 exposed vs *unc-49(e407);aijSi2[Pges-1::unc-49]* PA14 exposed	1	
ins-20	WT OP50 fed vs *unc-49(e407)* OP50 fed	1	Fig. S5A
	WT OP50 fed vs WT PA14 exposed	0.1771	
	WT PA14 exposed vs *unc-49(e407)* PA14 exposed	1	
ins-27	WT OP50 fed vs *unc-49(e407)* OP50 fed	1	Fig. S5B
	WT OP50 fed vs WT PA14 exposed	0.1659	
	WT PA14 exposed vs *unc-49(e407)* PA14 exposed	0.7094	
ins-19	WT vs *ins-19(tm5155)*	6.0×10^{-6}	Fig. S6B
ins-31	WT vs *ins-19(tm5155)*	0.0535	
ins-19	WT vs *ins-31(ok3543)*	0.1227	Fig. S6C
ins-31	WT vs *ins-31(ok3543)*	0.0009	

Table S3. The primers of the examined genes for quantitative real-time PCR.

Target gene	Forward primer sequence	Reverse primer sequence	Note
tba-1	TCAACACTGCCATCGCCGCC	TCCAAGCGAGACCAGGCTTCAG	Internal control gene.
abf-2	GCTGCCGACATCGACTTTA	CGACCGCTTCGTTTCTTGC	Insulin-like signaling/*daf-16* pathway dependent gene.
ctl-2	CTACAGTCGGTGGTGAGAGC	TCGGGAAGTGGATAGGGTCA	IIS/*daf-16* pathway dependent gene.
dod-22	CCAGGATACAGAATACGT	CCAGAGATGACTTCAGTT	IIS/*daf-16* pathway dependent gene.
mtl-1	TGCGGAGACAAATGTGAATG	GCTTCTGCTCTGCACAATGA	IIS/*daf-16* pathway dependent gene.
sod-3	CTACTGCTCGCACTGCTTCA	ATCTGGGAGAGTGTGCTTGG	IIS/*daf-16* pathway dependent gene.
thn-1	TCTCGCTCTCCTGCTTTTGG	CAGCCGTAAGTTGGAAGCCT	IIS/*daf-16* pathway dependent gene.
F35E12.5	ACACAATCATTTGCGATGGA	GGTAGTCATTGGAGCCGAAA	*pmk-1* pathway dependent gene.
F08G5.6	TGGACAACCCAGATATGCAA	GTATGCGATGGAAATGGACA	*pmk-1* pathway dependent gene.
K08D8.5	TTACGATGGTGATTCCGT	GCTTGTTGCCAGTTGAGA	*pmk-1* pathway dependent gene.
lys-1	TTCGGATCTTTCAAGAAG	TGGGATTCCAACAACGTA	*pmk-1* pathway dependent gene.
lys-2	ATCGACTCGAACCAAGCTGCG	TCGACAGCATTTCCCATTGAAGCGT	*pmk-1* pathway dependent gene.
clec-85	CCTGATGATAAGTATATT	GGTTTTGGCTGTAGCACG	*pmk-1* pathway dependent gene.
ins-31	GTTTGCCAGACCGGAGAAAA	TTGATGTCTTCACCGCACAC	Insulin-like peptide INS-31 coding gene.
ins-20	GCTCGAATGTTGATGATAACCT	TTCATTCTGGACAGCACCGT	Insulin-like peptide INS-20 coding gene.
ins-27	GCCGCTTAATTCCCTATGTCTA	GACAGCAAGCCTTTTGGACTT	Insulin-like peptide INS-27 coding gene.
ins-19	AGAGTATGCGTGAAGGATATAGATC	ACTTCCTCACTGCAAATATGCTTC	Insulin-like peptide INS-19 gene.

SI materials and methods

Experimental *C. elegans* animals. Strains were maintained at 20 °C with standard procedures unless otherwise specified on nematode growth media (NGM) plates seeded with *Escherichia coli* OP50 as a food source (1). The Bristol strain *C. elegans* N2 was used as wild-type. Strains were maintained at 20 °C then shifted to 25 °C for *P. aeruginosa* PA14 lawn avoidance assays and pathogenesis survival assays.

The following mutant alleles and transgenes were used in this study:

LGI: *unc-29(kr29::tagRFP)* (2), *daf-16(mu86)*. LGII: *krSi2[Punc-49::unc-49::tagRFP]* (3), *age-1(hx546)*, *nsy-1(ag3)*, *ins-19(tm5155)*, *ins-31(ok3543)*, *juIs1;ins-31(ok3542)*, *krSi2;ins-31(ok3542)*, *oxIs22[Punc-49::unc-49::GFP+lin-15(+)](4)*. LGIII: *unc-25(e156), unc-47(n2409)*, *unc-49(e382)*, *unc-49(e407)*, *daf-2(e1370)*. LGIV: *unc-30(e191)*, *unc-30(hzhCR1::GFP)* (5), *juIs1[P_{unc-25}::snb-1::GFP]*(6), *gbb-2(tm1165)*, *pmk-1(km25)*. LGX: *gbb-1(tm1406)*, *sek-1(km4), lin-15AB(n765ts).* Integrants: *zIs356[daf-16::GFP + rol-6(su1006)], unc-49(e407);zIs356, unc-30(e191);zIs356, ins-31(ok3543);zIs356. muIs61[daf-16::GFP + rol-6(su1006)], unc-49(e407);muIs61, unc-30(e191);muIs61, ins-31(ok3543);muIs61.* Transgenes: *krEx1068[Pmadd-4^{fosmid}::madd-4L::GFP] and krEx1069[Pmadd-4^{fosmid}::madd-4B::GFP]* (3). Double mutant alleles: *unc-49(e407);daf-16(mu86)*, *unc-49(e407);daf-2(e1370)*, *unc-49(e407);age-1(hx546)*, *unc-49(e407);pmk-1(km25)*, *unc-49(e407);nsy-1(ag3)*, *unc-49(e407);sek-1(km4)*, *unc-49(e407);ins-31(ok3543), unc-30(e191);daf-2(e1370).*

The following transgenic lines and single-copy insertion transgenes were created in this study:

In *unc-25(e151);lin-15AB(n765ts)* worms: *aijEx41*, *aijEx42*, *aijEx43[pKN03; pEKL15]*, *aijEx44, aijEx45, aijEx46[pHP03; pEKL15], aijEx143[Punc-30::unc-25], aijEx181[Punc-30::unc-30]*.

In *unc-49(e407);lin-15AB(n765ts)* worms: *aijEx21[pXZ06; pEKL15]*, *aijEx22[pXZ05; pEKL15]*, *aijEx109*, *aijEx110[pHP31; pEKL15]*, *aijEx87*, *aijEx88[pHP24; pEKL15]*, *aijEx89, aijEx90[pHP25; pEKL15]*, *aijEx111, aijEx112, aijEx113[pHP32; pEKL15]*.

In *ins-31(ok3543);lin-15AB(n765ts)* worms: *aijEx125*, *aijEx126, aijEx127[pHP24; pEKL15]*, *aijEx130*, *aijEx131*, *aijEx132[pHP25; pEKL15]*, *aijEx135, aijEx136, aijEx137[pHP31; pEKL15]*.

In *lin-15AB(n765ts)* worms: *aijEx157*, *aijEx158*, *aijEx159[pSY03*; *pSY04*; *pEKL15].*

Single-copy insertion alleles in *ttTi5605* locus of ChrII: *aijSi1[pXZ05, Pmyo-3::unc-49::tagRFP::unc-54 3' UTR]*, *aijSi2[pXZ06, Pges-1::unc-49::tagRFP::unc-54 3' UTR]*, *aijSi12[pSY01, Punc-30::Tetx::SL2::GFP::unc-54 3' UTR]*.

Germline transformation. Transformation was conducted by microinjection of plasmid DNA into the gonad of *C. elegans* young adult animals as described (7). Transgenic lines were based on the rescue of *lin-15AB(n765ts)* at 20 °C or 25 °C otherwise stated specifically.

For specific rescue of *unc-49(e407)* mutant by UNC-49 (3, 4), pXZ05, or pXZ06 was injected at 10 ng μl^{-1} with pEKL15(*lin15(+)*) at 20 ng μl^{-1} and 1 kb ladder (New England Biolabs) up to 100 ng μl^{-1}, respectively.

For endogenous and specific rescue of *unc-25(e156)* mutant, pHP03(*Punc-25::unc-25::SL2::GFP*), or pKN03(*Punc-47$_{(truncated)}$::unc-25::SL2::GFP*), pHP28(*Punc-30::unc-25::SL2::GFP::unc-54 3'UTR*), or pJL24(*Punc-30::unc-30::SL2::GFP::unc-54 3'UTR)* was injected at 20 ng μl^{-1} with pEKL15(*lin15(+)*) at 20 ng μl^{-1} and 1kb ladder up to 100 ng μl^{-1}.

For endogenous and specific rescue of *ins-31(ok3543)* or *unc-49(e407)* mutant by INS-31, pHP24, pHP25, pHP31, or pHP32 was injected at 30 ng μl^{-1} with pEKL15(*lin15(+)*) at 10 ng μl^{-1} and 1 kb ladder up to 100 ng μl^{-1}.

For *ins-31* expression pattern, pSY03 was injected at 30ng μl^{-1}, pSY04 at 20ng μl^{-1} wtih pEKL15 at 10 ng μl^{-1} and 1 kb ladder up to 100 ng μl^{-1}.

Generation of single-copy insertion alleles by homologous recombination. The *aijSi1* and *aijSi2* alleles encode UNC-49 fused with red fluorescent protein tagRFP (UNC-49-tagRFP) mini-gene under the control of muscle-cell-specific *myo-3* or intestine-specific *ges-1* promoter, respectively, and were generated by using the Mos1-mediated single-copy insertion (*MosSCI*) technique as described(8). The UNC-49-tagRFP mini-gene composed of a genomic DNA fragment containing the first four exons of unc-49, a cDNA fragment corresponding to the last eight exons of unc-49B isoform and the 3' UTR sequence of *unc-54*, was amplified from pHT22.1 plasmid. The

2.7 kb of specific muscle promoter P*myo-3* and the 2.5 kb of specific intestine promoter P*ges-1* were amplified from genomic DNA of wild-type strain N2, respectively. The pXZ05 or pXZ06 repair template was injected at 42.5 ng μl^{-1} with pCFJ601($P_{eft\text{-}3}$*::Mos1 transposase*) at 50 ng μl^{-1}, the pMA122 negative selection marker at 10 ng μl^{-1}, pGH8 at 10 ng μl^{-1}, pCFJ90 at 2.5 ng μl^{-1}, pCFJ104 at 5 ng μl^{-1}, and 1 kb ladder (New England Biolabs) up to 120 ng μl^{-1} into *unc-119(ed3)III; ttTi5605 II* animals picked from EG6699 strain.

The *aijSi12* allele encodes the light chain of tetanus toxin (TeTx) used to inhibit chemical synaptic transmission (9, 10) under the control of GABAergic D-type motor neurons promoter *unc-30* (*Punc-30::TeTx::SL2::GFP*) in wild-type worms was generated by *MosSCI*. The sequence of TeTx gene was amplified from the plasmid gifted from Dr. S. Gao (11). The *unc-30* promoter sequences were derived from pXZ05 plasmid. The fragment of *Punc-30::TeTx::SL2::GFP* fused with the 3' UTR sequence of *unc-54* was inserted into pCFJ151 at *Xho*I and *Spe*I sites by using isothermal assembly(12). The uncoordinated moving animal picked from EG6699 strain was injected with pSY01.

Plasmid construction. The plasmids were built by using isothermal assembly (12), otherwise stated specifically else. The following plasmids were created in this study:

pXZ05: *Pmyo-3::unc-49::tagRFP::unc-54 3' UTR*. The 2.7 kb fragment of muscle specific promoter P*myo-3* was amplified from genomic DNA of wild-type strain N2 and the *unc-49-tagRFP::unc-54 3' UTR* mini-gene was amplified from pHT22 plasmid (13). The fragments of P*myo-3* fused with *unc-49::tagRFP::unc-54 3' UTR* mini-gene was inserted into pCFJ151 vector at *Spe*I and *Xho*I sites.

pXZ06: *Pges-1::unc-49-tagRFP::unc-54 3' UTR*. The 2.5 kb fragments of intestine specific promoter P*ges-1* was amplified from genomic DNA of wild-type strain N2, and *unc-49::tagRFP::unc-54 3' UTR* mini-gene was amplified from pHT22 plasmid (13). The fragments of *Pges-1* fused with *unc-49-tagRFP::unc-54 3' UTR* mini-gene was inserted into pCFJ151 vector at *Spe*I and *Xho*I sites.

pNK03: *Punc-47$_{truncated}$::unc-25::SL2::GFP::unc-54 3'UTR*. The 190 bp fragment of *unc-47* truncated promoter (*Punc-47$_{truncated}$*) (14) and 7,054 bp genomic DNA fragment of *unc-25* coding region (from initiation codon ATG to stop codon TAA) were amplified from N2 genomic DNA fused with *SL2::GFP* sequence derived from pNP403 plasmid and *unc-54 3'UTR* region were inserted into pJET1.2 vector (CloneJET PCR Cloning kit, Thermo Scientific, K1232#) by using isothermal assembly(12). *Apa*I site was introduced between genomic DNA fragment of *unc-25* coding and *SL2-GFP* sequence regions.

pHP03: *Punc-25::unc-25::unc-25 3'UTR*. The sequence of *unc-25* locus containing 2,116 bp promoter region, 7,054 bp genomic DNA sequence of UNC-25 coding region, and 867 bp *unc-25* 3' UTR region was amplified from genomic DNA of wild-type strain N2 and then inserted into pJET1.2.

pHP24: *Pges-1::ins-31::SL2::GFP::unc-54 3'UTR.* The 2.5 kb fragment of intestine promoter P*ges-1* derived from pXZ06 and the genomic DNA sequence of *ins-31* coding sequence amplified from genomic DNA of wild-type strain N2 were fused and inserted into pNK03 vector at *Not*I and *Apa*I sites, in which the fragment of *Punc-47$_{truncated}$::unc-25* was removed.

pHP25: *Pmyo-3::ins-31::SL2::GFP::unc-54 3'UTR.* The 2.7 kb fragment of muscle specific promoter P*myo-3* was derived from pXZ05 and the genomic DNA sequence of *ins-31* coding sequence amplified from genomic DNA of wild-type strain N2 were fused and inserted into pNK03 vector at *Not*I and *Apa*I sites, in which the fragment of *Punc-47$_{truncated}$::unc-25* was removed.

pHP28: *Punc-30::unc-25 ::SL2 ::GFP::unc-54 3'UTR*. The 2,627 bp sequence of D type motor neuron promoter P*unc-30*, and *unc-25* cDNA and *SL2::GFP::unc-54 3'UTR* sequence from pNK03 were inserted into *Xho*I and *Spe*I sites of pCFJ151 vector.

pJL24: *Punc-30::unc-30 ::SL2 ::GFP ::unc-54 3'UTR.* The 2,627 bp sequence of D type motor neuron promoter Punc-30, and *unc-30* cDNA and *SL2::GFP::unc-54 3'UTR* sequence from pNK03 were inserted into *Xho*I and *Spe*I sites of pCFJ151 vector.

pGJ07*: ins-19ins-31 loci::SL2::GFP::unc-54 3'UTR*. The genomic DNA sequence of *ins-31* and *ins-19* loci amplified from genomic DNA of wild-type strain N2 was inserted into pNK03 vector at *Not*I and *Apa*I sites, in which the fragment of *Punc-47$_{truncated}$::unc-25* was removed.

pHP31: *Pins-31::ins-31::SL2::GFP::unc-54 3'UTR.* The sequence with the deletion of the *ins-19* coding region was amplified by reverse PCR strategy and using pGJ07 as a template, and then was self-fused using isothermal assembly(12).

pHP32: *Pins-19::ins-19::SL2::GFP::unc-54 3'UTR.* The sequence with the deletion of the *ins-31* coding region was amplified by reverse PCR strategy and using pGJ07 as a template, and then was self-fused.

pSY01: *Punc-30::Tetx::SL2::GFP::unc-54 3'UTR.* The 2,627 bp sequence of D type motor neuron promoter P*unc-30*, and Tetx sequence(11) and *SL2::GFP::unc-54 3'UTR* sequence from pNK03 were inserted into *Xho*I and *Spe*I sites of pCFJ151 vector.

pSY03: $P_{ins\text{-}31}$*::NLS::YFP*. The 599bp promoter of *ins-31* derived from pHP31 was inserted into the *Hind*III and *Xba*I sites of pPD133.97 (L4687, Fire kit) vector, in which the *myo-3* promoter sequence was removed.

pSY04: $P_{myo\text{-}3}$*::NLS::mCherry*. The 864 bp encoding sequence of mCherry amplified from pCFJ90 was inserted into the *Age*I and *Nhe*I sites of pPD133.97 (L4687, Fire kit) vector, in which the GFP encoding sequence was removed.

pJL09: P_{CMV}*::ins-31::GFP*. The 657 bp *ins-31* cDNA amplified from total RNA of wild-type strain N2 by reverse transcription polymerase chain reaction (RT-PCR) and the GFP sequence derived from pBP38(3) was fused by fusion PCR strategy, which then was inserted into pCEP4 vector (Thermo-Fisher Scientific) at *Not*I and *Kpn*I sites. This plasmid was used to perform co-immunoprecipitation in transfected HEK 293T cells.

pJL10: P_{CMV}*::SP::GFP*. The 48 bp signal peptide sequence of *ins-31* amplified from pJL09 and the GFP sequence derived from pBP38 (3) was fused by fusion PCR strategy, which then was inserted into pCEP4 vector (Thermo-Fisher Scientific) at *Not*I and *Kpn*I sites. This plasmid was used to perform co-immunoprecipitation in transfected HEK 293T cells.

pJL11: P_{CMV}*::daf-2::3×Flag*. The extracellular region coding sequence (3,552bp) of *daf-2* amplified from total RNA of wild-type strain N2 by RT-PCR with the 3' terminal end primer containing the coding sequence of three Flag repeats (3×Flag) was inserted into pCEP4 vector at *Not*I and *Kpn*I sites. This plasmid was used to perform co-immunoprecipitation in transfected HEK 293T cells. All plasmids were verified by sequencing and available from the authors on request.

***C. elegans* killing assay.** The killing assay by *P. aeruginosa* PA14 was performed as previously described (15) with minor modifications. Briefly, the overnight cultured *P. aeruginosa* PA14 was seeded on modified NGM (0.35% instead of 0.25% peptone) in 3.5 cm-diameter plates to cover the full surface of NGM agar, namely slow killing assay plates. The slow-killing assay plates were incubated at 37 °C for 24 h after dried at room temperature, and then shifted to balance the temperature at 25 °C for 8-12 h prior to seeding with synchronized larval L4 stage animals. The slow-killing assays were performed at 25 °C. Animals were scored for survival per twelve hours and transferred to fresh slow-killing assay plates daily. Animals were considered dead if they failed to respond to the repeated touch of a platinum wire. 50 μg ml^{-1} 5-Fluoro-29-deoxyuridine (FUdR, Sigma, F0503) was included in the slow-killing assay NGM to prevent the growth of progeny and "bagging". Fifty animals were used for each experiment and those that died of vulva burst or crawling off plates were censored. All survival experiments were performed at least three independent replicates. For the killing assay by *S. aureus*, the overnight cultured bacteria were diluted at 1:5, then seeded on 3.5 cm-diameter tryptic soy agar (Aobox, 02-102) plates containing 5 μg ml^{-1} naladixic acid (Macklin, 3374-05-8). Plates were incubated at 37 °C for 6 h, shifted to balance the temperature of the plates at 25 °C for 2-4 h, and then used to perform the killing assay by *S. aureus*, of which the following steps were the same as the slow-killing assay by *P. aeruginosa* PA14 described above.

***P. aeruginosa* PA14 avoidance assay.** The PA14 avoidance assay was performed with minor modification as described (16). A 20 μL drop of *P. aeruginosa* PA14 culture was seeded on 6.0 cm NGM plates and cultured at 37 °C for 24 h. Thirty larval L4 nematodes were transferred to the centre of each PA14 lawn on the modified NGM plate. The number of nematodes was counted at 2, 4, 6, 8, and 10 h post-exposure for presence or absence on each PA14 lawn.

Lifespan assay on heat-killed *P. aeruginosa* PA14. Lifespan assay on heat-killed *P. aeruginosa* PA14 was carried out as previously described (16). Briefly, bacteria were concentrated 1:5 and heat-killed at 65 °C for 3 hours. The death of *P. aeruginosa* PA14 was confirmed by falling to grow on Luria-Bertani (LB) plates at 37 °C overnight. Heat-killed *P. aeruginosa* PA14 was seeded on a 3.5 cm plate of modified NGM containing 50 μg ml^{-1} FUdR and 50 μg ml^{-1} ampicillin (Sangon Biotech, A610028). The Synchronized larval L4 worms were moved to the heat-killed PA14 plates. Animals were scored for survival daily and transferred to fresh plates per 2-3 days. Animals were considered dead if they failed to respond to the repeated touch of a platinum wire.Those that died of vulva burst or crawling off plates were censored. The assay was performed at 25 °C.

Quantification of intestinal *P. aeruginosa* PA14 loads. The quantification of colony forming units (CFU) was modified from the previous description (16). The worms were exposed to *P. aeruginosa* PA14 for 24 h in the same conditions as the killing assay. Ten nematode animals were transferred to M9 solution containing 100 mM sodium azide (Amersco, 0639) to paralyze the worm and stop the pharyngeal pumping, washed three times with an antibiotic M9 solution containing 1 mg ml^{-1} ampicillin (Sangon Biotech, A610028) and 1 mg ml^{-1} gentamicin (Solarbio, G8170), followed by 30 min of incubation in the antibiotic solution to kill the bacteria present on the exterior of worms. The worms were lysed with a motorized pestle after transferred onto new NGM plates containing 1 mg ml^{-1} ampicillin and 1 mg ml^{-1} gentamicin for another 30 min to further eliminate the external PA14. Serial dilutions of the lysates (10^{-1}, 10^{-2}, 10^{-3}, 10^{-4}) were plated onto LB plates containing 100 μg ml^{-1} rifampicin (Solarbio, R8011) to select for PA14 and grown overnight at 37 °C. The colonies of PA14 were counted to determine CFU per worm. At least three independent replicates were performed.

Behavioral analysis. The pharyngeal pumping was counted manually by visual inspection of movies taken with DIC optics using a Multi-Purpose Zoom Microscope (AZ100, Nikon) and played at slow speed. One movement sequence consisting of an opening and a closing of the terminal bulb (TB) was counted as one pumping movement. The number of pharyngeal pumping was counted within one minute. To determine the percentage of successful enteric muscle contractions per defecation cycle, we scored for the presence of an enteric muscle contraction following a posterior body contraction (EMC/pBoc). Ten defecation cycles from individual young adult animals were scored for each genotype (17, 18). Three times of experiments were performed independently.

Visualization of bacterial accumulation assay. Overnight cultures of *P. aeruginosa* expressing GFP (PA14::GFP) were seeded on slow-killing NGM plates and incubated at 37 °C for 24 h. Synchronized larval L4 worms were transferred to the plates and cultured at 25 °C for indicated times after PA14::GFP exposure. Before the examination of bacterial accumulation in the intestine and the pharyngeal lumen of animals, worms were washed in M9 buffer to eliminate the fluorescent bacteria stuck to the cuticle of worms. Animals were visualized using a Multi-Purpose Zoom Microscope (AZ100, Nikon). The intensity of fluorescence was analyzed using ImageJ software (v1.8.0, NIH).

Green fluorescent bead intake assay. The assay was performed by feeding the worms with mixtures of OP50 or PA14 bacteria and 0.5-μm green fluorescent polystyrene beads (Phosphorex, Inc., 2103A) (19). The overnight cultured *E. coli* OP50 or *P. aeruginosa* PA14 were mixed with the fluorescent beads at a ratio of 25:1 and 100 μl of the mixtures were seeded onto the 35 mm-diameter NGM plates, and incubated at 37 °C for 24 h. Synchronized young adult worms were transferred to the plates and incubated at 25 °C for 2 h. The worms were washed in M9 buffer with 25 mM sodium azide to remove the fluorescent beads that adhere to the body surface, following by being mounted to the Multi-Purpose Zoom Microscope (AZ100, Nikon). The fluorescence intensity of the area containing the GFP fluorescent beads was analyzed using ImageJ software (v1.8.0, NIH).

RNA isolation. Synchronized larval L1 worms were transferred onto NGM plates seeded with OP50 and grown at 20 °C till the worms reached larval L4 stage. Animals were collected, quickly washed once with M9 solution, and then transferred to modified NGM plates seeded with OP50 or PA14, cultured at 25 °C for 24 h. Animals were washed off the plates and rinsed once with M9 solution. The worm pellet was re-suspended in TRIzol (Transgen, ER501-01-01) for total RNA extraction or frozen at -80 °C for future experiments. Total RNA was obtained using TransZol Up Plus RNA Kit (Transgen, ER501-01) and cDNAs were synthesized by using the kit of TransScript All-in-One First-Strand cDNA Synthesis SuperMix (Transgen, AT341-02), made aliquots and frozen at -80 °C for subsequent experiments.

Quantitative real-time PCR (qRT-PCR). Total RNA was obtained as described above. qRT-PCR was performed using SYBR PCR Master Mix (Transgen, AQ141-02) on a Bio-Rad CFX96 real-time PCR machine. Relative fold-changes for transcripts were calculated using comparative C_T ($2^{-\Delta\Delta CT}$) method and normalized to *tba-1* gene encoding a tubulin. All experiments were performed at least three times independently. The primers used to examine the target genes were listed in **Table S3**.

RNA interference. RNAi was performed by feeding worms with *E. coli* strain HT115 (DE3) expressing double-strand RNA homologous of target genes as described (20). HT115 (DE3) was grown overnight in LB broth containing 100 μg ml^{-1} ampicillin (Sangon Biotech, A610028) at 37 °C and spread onto NGM plates containing 100 μg ml^{-1} ampicillin and 2 mM isopropyl 1-thio-β-D-galactopyranoside (IPTG, Sangon Biotech, A600168). The worms were allowed to grow about 24 h at room temperature on the NGM plates seeded with *E. coli* strain HT115 (DE3) expressing indicated RNAi. L2-L3 larval worms of indicated genotype strains were seeded onto RNAi plates and cultured for 2 days at 20 °C. The gravid adults were then transferred onto fresh bacterial lawns expressing indicated RNAi and allowed to lay eggs for 2 h to obtain RNAi-animal population of the second generation. The eggs were allowed to develop to reach larval L4 stage for subsequent experiments at 20 °C.

Imaging and fluorescence quantification. Images were acquired using a Nikon Ti-E Inverted Confocal Microscope equipped with a Princeton Instruments PIXIS 400B Digital CCD Camera System. For the quantitative analysis of GABAergic presynaptic bouton (*juIs1*, SNB-1::GFP) (6) and post-synaptic $GABA_AR$ (*krSi2*, *Punc-49::unc-49::RFP*)(13), L-AChR (*kr208[unc-29::RFP]*) (2), or MADD-4L::GFP (*krEx1068[Pmadd-4$_{fosmid}$::madd-4L::GFP]*) (3), MADD-4B::GFP (*krEx1069[Pmadd-4$_{fosmid}$::madd-4B::GFP]* (3) fluorescence in living worms, young adult animals were mounted on 2% agarose pads and immobilized using 0.1 M sodium azide (Sigma) in M9 buffer and pictures of dorsal cords were acquired as described previously(13). Acquisition settings were the same across genotypes for quantitative analysis. For evaluating the fluorescence level in different genetic backgrounds, each genotype was analysed on three different days, and the data were pooled together. Data are presented as a percentage of the mean fluorescence relative to that of the wild-type. All results of fluorescence quantification are presented as means and s.e.m..

Electrophysiology. Electrophysiological recording was done on dissected *C. elegans* as previously described (21, 22). Briefly, the larval L4 late stage hermaphrodite animals were glued to a sylgard-coated glass which was covered with bath solution in a chamber after fed on *E. coli* OP50 or exposed to *P. aeruginosa* PA14 for 24 h at 25 °C. Anterior body wall muscle cells were patched by fire-polished 4–6 MΩ resistant borosilicate, which were pulled by a P-1000 puller (Sutter Instruments, Novato, CA, USA). mIPSCs were recorded in the whole-cell configuration by HEKA EPC9 amplifier (HEKA, Lambrecht, Germany), using the Pulse software (HEKA Elektronik). Data were sampled at 10 kHz. Solutions for mIPSCs recording were described in the previous study(22). Specifically, the intracellular solution contained (in mM): 115 K-gluconate; 25 KCl; 0.1 $CaCl_2$; 5 $MgCl_2$; 1 BAPTA; 10 HEPES; 5 Na_2ATP; 0.5 Na_2GTP; 0.5 cAMP; 0.5 cGMP, pH 7.2 adjusted by KOH, ~320 mOsm. The extracellular solution contained (in mM): 150 NaCl; 5 KCl; 5 $CaCl_2$; 1 $MgCl_2$; 10 glucose; 5 sucrose; 15 HEPES, pH 7.2 adjusted by NaOH, ~330 mOsm. As previously reported, the reversal potentials of GABARs and AChRs were -30 mV (22) and +20 mV (23), respectively. The recording potential was held at -10 mV, with ionotropic acetylcholine receptor blocker D-

tubocurarine (d-TBC, 0.5 mM) included in the extracellular solution to isolate mIPSC events at GABAergic NMJs of worms. All the chemicals were purchased from Sigma Aldrich. All the recordings were conducted at 22 °C.

Cell culture and Transfection. Human embryonic kidney (HEK) 293T cells (ATCC, CRL-11268) were maintained in Dulbecco's modified Eagle's medium with 10% inactive fetal bovine serum and penicillin-streptomycin (Gibco, Grand Island, 15140122) at 37 °C supplied with 5% CO_2 in an incubator (Thermo Fisher Scientific) with a humidified atmosphere as described previously (24). The cells were washed once using PBS and digested with 0.05% Trypsin-EDTA (Gibco, Grand Island, 25300054) at 37 °C for routine passage of the cells. HEK 293T cells were transiently transfected with indicated constructions using the polyethylenimine (PEI, 1 mg/ml in ddH_2O) reagent (Polyscience, 24765-2). The PEI/DNA mixture with the ratio of PEI to DNA at 3:1 was incubated for 30 min at room temperature before added to the HEK 293T cell cultures dropwise.

Biochemistry. Co-immunoprecipitation (Co-IP) were performed as previously described (13). Briefly, 10 ml of the cell culture supernatants of HEK 293T cells transiently transfected with indicated constructions in the plates of diameter at 10 cm were harvested at around 48 hours post-transfection, centrifuged to remove the cell debris (13,000 rpm, 10 min at 4 °C), and then 500 µL of 1 M HEPES (pH 7.7) was added to buffer the pH value. For the Co-IP of SP::INS-31::GFP or SP::GFP and three Flag repeats tagged extracellular domain of DAF-2 (DAF-2Ecto::3xFlag), the prewashed 20 µl of anti-GFP-Trap-A beads (Chromotek, gta-20) was added and incubated overnight at 4 °C with gentle rotation. The anti-GFP-Trap-A beads were collected by centrifugation at 1,000 g for 3 min at 4 °C. The beads were washed six times with ice cold immunoprecipitation (IPB, 50 mM HEPES, pH7.7, 100 mM NaCl, 50 mM KCl, 2 mM $MgCl_2$, 1 mM EDTA, 1 µg/ml pepstatin, 1 µg/ml leupeptin, 2 µg/ml aprotinin, 1mM PMSF, 1 tablet of protease inhibitor cocktail per 10 ml buffer) buffer containing 0.05 % Triton X-100. After last time wash, the beads were re-suspended by 60 µl IPB buffer, the immunoprecipitated proteins were eluted in 3 × laemmli buffer with beta-mercaptoethanol, and analyzed by western blotting after boiled for 10 min at 98 °C. For the western blotting, the primary anti-GFP Rabbit polyclonal antibody (Invitrogen, A-11122) at a 1:3,000 dilution or anti-Flag mouse monoclonal antibody (MBL, M185-3L) at a 1: 12,000 dilution was used, and horseradish peroxidase (HRP)-conjugated goat anti-rabbit (Transgen, HS101-01) or anti-mouse (Transgen, HS201-01) was used as secondary antibody at a 1:2,000 or 1:5,000 dilution, respectively. The images of blotting membranes were captured by an imaging system (MicroChemi 4.2, DNR Bio Imaging Systems). All the co-immunoprecipitation experiments were repeated at least three times independently.

Nuclear localization analyses of DAF-16a^{AM}–GFP. To observe DAF-16 subcellular distribution, a stably integrated DAF-16::GFP transgenic allele *zIs356* (25, 26) and CF1139 (27) were introduced into *unc-49(e407), unc-30(e191),* and *ins-31(ok3543)* mutant. The well-fed larval L4 stage worms were mounted in M9 buffer containing 25 mM sodium azide on agar pad and imaged immediately using a Multi-Purpose Zoom Microscope (AZ100, Nikon). For *zIs356*, more than 100 animals for each genotype were used to evaluate and classified into three categories as nuclear, intermediate and cytoplasmic localization of DAF-16::GFP based on the accumulation intensity of GFP in the nucleus and the cytoplasm of the intestinal cells of each animal (28). For CF1139, considering the very low GFP signal, the anterior worm body were imaged and classified into two categories as nuclear and cytoplasmic localization on the basis of GFP signal could be visilized in the nucleus of animals (27).

ROS Detection. ROS determined by DCF-DA were detected as described in previous study (29) with minor modification. Briefly, approximately 1000 young adult worms were collected in M9 buffer, washed three times with M9, once with PBS. The worm extracts were prepared by sonication and subsequent centrifugation at 15,000 rpm at 4 °C. Supernatants containing 10 µg of protein was pre-incubated in PBS with 100 µM DCF-DA (Beyotime, S0033S) at 37 °C for 1 hour. Fluorescence intensity was measured with a fluoremeter (PerkinElmer, USA) at the excitation wavelength 488 nm and the emission wavelength 535 nm. Intestinal ROS determined by DHE staining as described previously (30). In brief, worms raised on agar plates were washed off with M9 buffer, and then

incubated in M9 buffer containing 3 μM DHE (Beyotime, S0063) for 30 min. After DHE buffer incubation, the worms were washed extensively in M9 buffer followed by imaging by using a Multi-Purpose Zoom Microscope (AZ100, Nikon). For scoring ROS signals, animals with signal present in both the anterior and posterior intestine were classified as "High"; animals with signal in only part of the intestine (anterior or posterior intestine, for instance) were classified as "Medium"; animals without or with very weak intestinal signal were classified as "Low".

Statistical analysis. Data were analyzed with Prism 8.0 (v8.4.3, GraphPad Software, Inc.) and SPSS® Statistics Version 25 (IBM, USA). For statistical analyses of all killing and life span assays, Log-rank (Kaplan-Meier) method was used to calculate p-values, which were listed in **Table S1**. For comparison of category of DAF-16–GFP subcellular localization (cytoplasm, intermediate, nuclear), a chi-square test was used. For comparison of two groups, an unpaired Student's *t* test was performed, otherwise a nonparametric Mann-Whitney test was performed for **Fig. 1e**, **1g**, **2d**, **2h**, **2i** and **Fig. S1c** and **1e** as these data of the samples were not normal distribution after being conducted by a D'Agostino & Person test. For the comparison of more than two groups, one-way ANOVA tests followed by Bonferroni's multiple comparison tests were performed. *p* value for all statistical analysis of quantitative RT-PCR are listed in **Table S2**.

SI references

1. Brenner S (1974) The genetics of Caenorhabditis elegans. *Genetics* 77(1):71-94.
2. Richard M, Boulin T, Robert VJ, Richmond JE, & Bessereau JL (2013) Biosynthesis of ionotropic acetylcholine receptors requires the evolutionarily conserved ER membrane complex. *Proc Natl Acad Sci U S A* 110(11):E1055-1063.
3. Pinan-Lucarre B*, et al.* (2014) C. elegans Punctin specifies cholinergic versus GABAergic identity of postsynaptic domains. *Nature* 511(7510):466-470.
4. Bamber BA, Beg AA, Twyman RE, & Jorgensen EM (1999) The Caenorhabditis elegans unc-49 locus encodes multiple subunits of a heteromultimeric GABA receptor. *J Neurosci* 19(13):5348-5359.
5. Yu B*, et al.* (2017) Convergent Transcriptional Programs Regulate cAMP Levels in C. elegans GABAergic Motor Neurons. *Dev Cell* 43(2):212-226 e217.
6. Zhen M & Jin Y (1999) The liprin protein SYD-2 regulates the differentiation of presynaptic termini in C. elegans. *Nature* 401(6751):371-375.
7. Mello CC, Kramer JM, Stinchcomb D, & Ambros V (1991) Efficient gene transfer in C.elegans: extrachromosomal maintenance and integration of transforming sequences. *EMBO J* 10(12):3959-3970.
8. Frokjaer-Jensen C*, et al.* (2008) Single-copy insertion of transgenes in Caenorhabditis elegans. *Nat Genet* 40(11):1375-1383.
9. Macosko EZ*, et al.* (2009) A hub-and-spoke circuit drives pheromone attraction and social behaviour in C. elegans. *Nature* 458(7242):1171-1175.
10. Schiavo G*, et al.* (1992) Tetanus and botulinum-B neurotoxins block neurotransmitter release by proteolytic cleavage of synaptobrevin. *Nature* 359(6398):832-835.
11. Guo M*, et al.* (2015) Reciprocal inhibition between sensory ASH and ASI neurons modulates nociception and avoidance in Caenorhabditis elegans. *Nat Commun* 6:5655.
12. Gibson DG (2011) Enzymatic assembly of overlapping DNA fragments. *Methods Enzymol* 498:349-361.
13. Tu H, Pinan-Lucarre B, Ji T, Jospin M, & Bessereau JL (2015) C. elegans Punctin Clusters GABA(A) Receptors via Neuroligin Binding and UNC-40/DCC Recruitment. *Neuron* 86(6):1407-1419.
14. Eastman C, Horvitz HR, & Jin Y (1999) Coordinated transcriptional regulation of the unc-25 glutamic acid decarboxylase and the unc-47 GABA vesicular transporter by the Caenorhabditis elegans UNC-30 homeodomain protein. *J Neurosci* 19(15):6225-6234.
15. Tan MW, Mahajan-Miklos S, & Ausubel FM (1999) Killing of Caenorhabditis elegans by Pseudomonas aeruginosa used to model mammalian bacterial pathogenesis. *Proc Natl Acad Sci U S A* 96(2):715-720.

16. Sun J, Singh V, Kajino-Sakamoto R, & Aballay A (2011) Neuronal GPCR controls innate immunity by regulating noncanonical unfolded protein response genes. *Science* 332(6030):729-732.
17. Beg AA & Jorgensen EM (2003) EXP-1 is an excitatory GABA-gated cation channel. *Nat Neurosci* 6(11):1145-1152.
18. Mullen GP*, et al.* (2006) The Caenorhabditis elegans snf-11 gene encodes a sodium-dependent GABA transporter required for clearance of synaptic GABA. *Mol Biol Cell* 17(7):3021-3030.
19. Cao X & Aballay A (2016) Neural Inhibition of Dopaminergic Signaling Enhances Immunity in a Cell-Non-autonomous Manner. *Curr Biol* 26(17):2398.
20. Timmons L & Fire A (1998) Specific interference by ingested dsRNA. *Nature* 395(6705):854.
21. Richmond JE & Jorgensen EM (1999) One GABA and two acetylcholine receptors function at the C. elegans neuromuscular junction. *Nat Neurosci* 2(9):791-797.
22. Gao S & Zhen M (2011) Action potentials drive body wall muscle contractions in Caenorhabditis elegans. *Proc Natl Acad Sci U S A* 108(6):2557-2562.
23. Maro GS*, et al.* (2015) MADD-4/Punctin and Neurexin Organize C. elegans GABAergic Postsynapses through Neuroligin. *Neuron* 86(6):1420-1432.
24. Jiang W*, et al.* (2015) An optimized method for high-titer lentivirus preparations without ultracentrifugation. *Scientific reports* 5:13875.
25. Henderson ST & Johnson TE (2001) daf-16 integrates developmental and environmental inputs to mediate aging in the nematode Caenorhabditis elegans. *Curr Biol* 11(24):1975-1980.
26. Lin K, Hsin H, Libina N, & Kenyon C (2001) Regulation of the Caenorhabditis elegans longevity protein DAF-16 by insulin/IGF-1 and germline signaling. *Nat Genet* 28(2):139-145.
27. Mouchiroud L*, et al.* (2013) The NAD(+)/Sirtuin Pathway Modulates Longevity through Activation of Mitochondrial UPR and FOXO Signaling. *Cell* 154(2):430-441.
28. Takahashi Y*, et al.* (2011) Asymmetric arginine dimethylation determines life span in C. elegans by regulating forkhead transcription factor DAF-16. *Cell Metab* 13(5):505-516.
29. Tang H & Pang S (2016) Proline Catabolism Modulates Innate Immunity in Caenorhabditis elegans. *Cell Rep* 17(11):2837-2844.
30. Wei Y & Kenyon C (2016) Roles for ROS and hydrogen sulfide in the longevity response to germline loss in Caenorhabditis elegans. *Proc Natl Acad Sci U S A* 113(20):E2832-2841.